

1 **Back to the bones: do muscle area assessment techniques predict functional evolution across a**
2 **macroevolutionary radiation?**

3
4 Karl T. Bates^{1*}, Linjie Wang², Matthew Dempsey¹, Sarah Broyde¹, Michael J. Fagan² & Philip G.
5 Cox^{3,4}.

6
7 ¹Department of Musculoskeletal Biology, Institute of Aging and Chronic Disease, University of
8 Liverpool, The William Henry Duncan Building, 6 West Derby Street, Liverpool L7 8TX, UK;

9 ²Department of Engineering, University of Hull, Hull, HU6 7RX, UK.

10 ³Department of Archaeology, University of York, PalaeoHub, Wentworth Way, Heslington, York
11 YO10 5DD, UK

12 ⁴Hull York Medical School, University of York, Heslington, York YO10 5DD, UK

13

14

15 *Correspondence to: k.t.bates@liverpool.ac.uk.

16 **Key words:** macroevolution, biomechanics, multi-body dynamics, finite element analysis, rodent

17 mastication

18 **SUMMARY**

19 Measures of attachment or accommodation area on the skeleton are a popular means of rapidly
20 generating estimates of muscle proportions and functional performance for use in large-scale
21 macroevolutionary studies. Herein we provide the first evaluation of the accuracy of these muscle
22 area assessment (MAA) techniques for estimating muscle proportions, force outputs and bone
23 loading in a comparative macroevolutionary context using the rodent masticatory system as a case
24 study. We find that MAA approaches perform poorly, yielding large absolute errors in muscle
25 properties, bite force and particularly bone stress. Perhaps more fundamentally, these methods
26 regularly fail to correctly capture many qualitative differences between rodent morphotypes,
27 particularly in stress patterns in finite element models. These findings cast doubts on the validity of
28 these approaches as means to provide input data for biomechanical models applied to understand
29 functional transitions in the fossil record, and perhaps even in taxon-rich statistical models that
30 examine broad-scale macroevolutionary patterns. We suggest that future work should go back to the
31 bones to test if correlations between attachment area and muscle size within homologous muscles
32 across a large number of species yield strong predictive relationships that could be used to deliver
33 more accurate predictions for macroevolutionary and functional studies.

34

35

36 **1. Introduction**

37 Calculation of the force-generating capacity of muscles, based on measurements of muscle
38 attachment sites and/or areas delineated by osteological structures, are widely used in
39 macroevolutionary studies of functional morphology and biomechanics [e.g. 1-27]. These muscle
40 area assessment (MAA) techniques have been applied to limbs [e.g. 22-24] and the axial skeleton
41 [e.g. 25-27] but are most frequently used in skulls (originating from the 'dry skull method' [1]) to
42 examine masticatory evolution in both extinct and extant taxa [e.g. 1-21]. For extinct taxa they
43 provide a means to derive quantitative estimates of muscle proportions, force output and bone
44 loading based on fossilised osteology alone, thereby circumventing the absence of muscle itself in
45 the fossil record. In extant taxa, extrapolating muscle size and mechanical performance from
46 existing bony specimens circumvents time-, labour- and skill-intensive physiological and
47 biomechanical experiments on live animals and/or cadavers, making it feasible to analyse large
48 sample sizes statistically and rapidly, and thus assess broad scale macroevolutionary patterns [e.g.
49 2-4,10,12,21]. Although rarely discussed explicitly as a benefit, this also minimises the need to
50 expose animals to experimentation and euthanasia, thus adhering to the principles of
51 the 3Rs (Replacement, Reduction and Refinement) in scientific research [28], assuming model
52 predictions are accurate enough to satisfy research goals.

53

54 However, the ability of MAA-based methods to accurately reconstruct qualitative and quantitative
55 functional patterns in a macroevolutionary radiation has not been extensively tested. To-date
56 measures of accuracy have largely been restricted to single taxon studies of muscle anatomy and
57 bite force [1, 29-34]. The varying levels of inaccuracy recovered by these studies contrasts
58 somewhat with a single comparative study of bats, which found that the method accurately
59 predicted bite forces despite inaccurately predicting muscle parameters [35]. In addition to the
60 limited assessment in explicit macroevolutionary contexts, to our knowledge, no study has
61 addressed the absolute or relative inaccuracy that MAA-based methods yield in finite element

62 studies of bone stress/strain, despite widespread combined use of these approaches. The extent to
63 which MAA reconstruction approaches accurately predict quantitative or even qualitative patterns
64 in macroevolutionary studies is therefore poorly constrained.

65
66 In this study we extend a recently published examination of soft tissue reconstruction and
67 biomechanical modelling in macroevolutionary studies [36] to MAA-based approaches to assess
68 quantitatively the capacity of these methods to correctly predict established differences between
69 macroevolutionary morphotypes. This not only allows us to assess the qualitative and quantitative
70 accuracy of MAA-based approaches, but also enables comparisons with alternative volumetric
71 sculpture methods widely used in palaeontological studies [e.g. 36-42].

72

73 **2. Material and Methods**

74 To assess the accuracy of MAA approaches we used the skeletal, multi-body dynamics analysis
75 (MDA) and finite element (FE) models of the grey squirrel (*Sciurus carolinensis*), brown rat (*Rattus*
76 *norvegicus*) and domestic guinea pig (*Cavia porcellus*) presented by Broyde et al. [36]. These taxa
77 are representative of masticatory morphotypes within the Rodentia (sciuriform, myomorph, and
78 hystricomorph), and have evolved disparate masticatory musculature and bite mechanics [43-47].
79 Models of these taxa allowed us to measure the accuracy of MAA approaches for predicting muscle
80 physiological cross-sectional area (PCSA), bite force and bone stress against model iterations that
81 use muscle force-generating properties directly measured through dissection and imaging [46-47].
82 These models, built using muscle parameters measured in the same specimens being modelled, are
83 referred to here as the ‘extant model’ iterations, as in Broyde et al. [36].

84

85 Here we investigated the accuracy of two MAA-based approaches: the dry skull method of
86 Thomason [1], which estimates the summed PCSAs of important muscle groups based on measures
87 of the accommodation space available for these muscles; and a potentially higher-resolution
88 approach in which PCSAs were estimated based on the bony attachment area (AA) of each
89 individual muscle. To measure individual muscle AAs in the models we used the already defined
90 attachment regions in the FE models (as in [36]; see ESM for more details) and these values were
91 used as the PCSAs for each muscle in the MDA models. For the dry skull model iterations, the
92 temporalis muscle PCSA input into the MDA models was set to the value derived from the MAA
93 for this muscle following Thomason [1], while the PCSA from the masseter + medial pterygoid
94 MAA was divided equally between the posterior line of action of the posterior deep masseter, the
95 anterior line of action of the superficial masseter and the medial pterygoids in the MDA model each
96 species. All other muscles were removed from the MDA models to reflect the aggregation of
97 muscle PCSA and force output into simplified temporalis and masseter + pterygoid groups (Fig S7).
98 In addition to incisor bite force, we also calculated the mechanical efficiency of bites as the ratio of
99 the bite force to the summed muscle forces, as done previously for these rodents by Cox et al. [46].
100 Predicted muscle forces from MDA models were then also used as inputs in the FE simulations. For
101 the dry skull FE models, muscle forces derived from the masseter + medial pterygoid MAA were
102 divided equally across the attachment sites of all masseter muscles and the medial pterygoids, while
103 the temporalis attachment area received the temporalis MAA derived force. All other muscle
104 attachment areas were not loaded, again to reflect the aggregation of muscle forces in the dry skull
105 method. All other parameters remained unaltered from the ‘extant iteration’ of models presented in
106 Broyde et al. [36,48].

107

108 **3. Results**

109 **(a) PCSA**

110 Both MAA approaches varied widely in the accuracy with which they estimated muscle PCSA in
111 the three rodent morphotypes (Fig 1a-b, Tables S1-4). The AA method gave similar average relative
112 error magnitudes per muscle in the three species (25-40%), but with considerable qualitative and
113 quantitative variation within individual muscles (Fig 1a, Table S1-3). In some cases, the AA
114 method gave similar errors in homologous muscles across the three morphotypes: the superficial
115 masseter PCSA was underestimated by 96-99.3% in the three morphotypes; error in the medial
116 pterygoid ranged from -78.2% to -96.3%; and the PCSA of the posterior deep masseter was
117 underestimated by 89% and 91.4% in the squirrel and rat (Fig 1a; Tables S1-3). However, other
118 muscles varied in both the nature and magnitude of error. For example, the temporalis predictions
119 yielded error of +694.5% and +171% in the squirrel and guinea pig compared to just +2.4% in the
120 rat. The AA method underestimated the PCSA of the posterior zygomatico-mandibularis in the
121 squirrel by 49.5% but overestimated it by 19.3% and 95.8% in the rat and guinea pig (Fig 1a,
122 Tables S1-3). These errors led to the AA approach correctly ordering taxa in the relative PCSAs of
123 homologous muscles only 10 out of 25 times (40%).

124

125 Similar error magnitudes and inconsistencies were recovered for the dry skull method (Fig 1b,
126 Table S4). Temporalis PCSA was overestimated by 110.5% in the squirrel but underestimated by
127 41.8% in the rat and just 0.2% in the guinea pig (Fig 1b, Table S4). However, the masseter + medial
128 pterygoid predictions all underestimated the real summed PCSAs of these muscles, by 28%, 46.4%
129 and 75.3% in the rat, guinea pig and squirrel. These errors led to the dry skull method correctly
130 ordering taxa in their relative PCSAs in 1 out of 6 cases.

131

132 ***(b) Bite force and mechanical efficiency***

133 When PCSAs derived from the AA and dry skull methods were used in MDA models, maximum
134 incisor bite forces were underestimated in all three species relative to the extant models: by 38.8%
135 in the squirrel, 21.8% in the guinea pig and 57.6% in the rat by the AA method, and by 76.7%,

136 64.5% and 51% by the dry skull method (Fig 2a-b, Table S5). These errors meant that the AA
137 iterations correctly identified the squirrel as having the highest bite force of the three morphotypes
138 but misclassified the guinea pig and rat relative to each other. The dry skull method predicts the
139 squirrel as having the lowest bite force rather than the highest but did correctly classify the rat as
140 having a higher bite force than the guinea pig (Fig 2a-b, Tables S5).

141

142 The AA and dry skull model iterations differ in the nature and magnitude of error they yield in
143 predictions of the mechanical efficiency of incisor biting across the rodent morphotypes (Fig 2c-d,
144 Tables S6-7). The AA model iterations underestimated mechanical efficiency in the rat and squirrel
145 by 11% and 21.7% but overestimated it by 7.6% in the guinea (Fig 2c-d, Tables S6-7). The dry
146 skull method underestimated mechanical efficiency in all three taxa, by 15.3% in the rat, 23.9% in
147 the squirrel and 25.6% in the guinea pig (Fig 2-d, Tables S6-7). Despite this error, the dry skull
148 method did maintain the correct qualitative differences between the three morphotypes seen in the
149 extant model iterations, with similarly high values of mechanical efficiency in the rat and squirrel
150 and lower efficiency in the guinea pig (Fig 2c, Table S6). However, the disparate nature of error in
151 the AA model predictions resulted in this iteration incorrectly identifying the squirrel with the
152 lowest mechanical efficiency (Fig 2c, Table S6).

153

154 **(c) Bone stress**

155 Here we focus on stress outputs from FE models (Fig 3) because tissue material properties in our
156 models were set to standardised generic and homogenous properties, mimicking the standard
157 approach in macroevolutionary studies [36]. For completeness, strain outputs across model
158 iterations are compared in the supplementary information. FE models loaded with muscle forces
159 derived from the MAA methods failed to capture many of the qualitative and quantitative patterns
160 in bone stress observed in the extant model iterations (Fig 3). With the exception of the guinea pig
161 AA model (Fig 3a, e) all MAA model iterations underestimate stress throughout the skulls: many

162 require an increase of ~50% to reach the stress magnitudes in the extant iterations, while the worse
163 performing models, such as the rat AA iteration (Fig 3a, e) require more than a 400% to match the
164 equivalent extant iteration. These large error magnitudes mean that both the AA and dry skull
165 models fail to correctly order the rodent macroevolutionary morphotypes in their relative stress
166 magnitudes. For example, the AA models suggest the rat experiences the lowest stress of the three
167 morphotypes instead of the highest, while the guinea pig is (at certain points along the skull)
168 recovered as experiencing the highest stresses rather than the lowest (Fig 3a, d-e). The dry skull
169 method also fails to recover the higher stresses expected in the squirrel versus guinea pig skull
170 across most of skull length (Fig 3b, e, f). Both MAA model types mostly capture the gross
171 qualitative changes in stress along skull length in the rat and guinea pig models (e.g. higher stresses
172 in the central skull length region associated with zygomatic arch). However, even gross changes in
173 stress distribution are poorly captured in the squirrel, particularly in the dry skull iteration where
174 mean regional stress remains consistently low across skull length (Fig 3).

175

176 **4. Discussion and Conclusions**

177 MAA-based approaches to estimate muscle size and force-generating capacity, and subsequently
178 bone loading, have been widely applied to extinct and extant taxa to examine the functional
179 consequences of changing morphology and macroevolutionary patterns in the locomotor, axial and
180 masticatory systems of vertebrates [e.g. 1-21]. Our study of its application to rodent masticatory
181 morphotypes builds upon a small number of previous evaluations of such approaches [1, 29-35] in a
182 number of ways: by extending assessment to FE models; by providing assessment of qualitative and
183 quantitative accuracy in an explicit macroevolutionary context; and by direct comparison to the
184 most widely used alternative method of numerical soft tissue reconstruction (volume sculpture [e.g.
185 36-42]).

186

187 Previous studies that have examined the accuracy of the dry skull method have suggested that the
188 approach overestimates the PCSA of the masseter muscles and medial pterygoid, while
189 underestimating the PCSA of the temporalis [1, 29-31]. Here we find a different pattern of error,
190 possibly owing to our taxonomic focus on rodents compared to that of previous evaluations of the
191 dry skull method, which used opossums, carnivorans and bats. In this analysis, the masseter +
192 medial pterygoid was underestimated by considerable amounts in all three rodent morphotypes, and
193 the temporalis PCSA was considerably overestimated in the squirrel, underestimated in the rat, but
194 accurately predicted in the guinea pig (Fig 1b).

195

196 We also recover a complex pattern of error at the individual muscle level in our AA-based estimates
197 (Fig 1, Tables S1-3). This approach underestimates PCSA in the superficial masseter, posterior
198 deep masseter and medial and lateral pterygoids and overestimates temporalis PCSA in all three
199 rodent morphotypes (Fig 1, Tables S1-3). However, the magnitude of this error varies enormously
200 across the three species (Fig 1a, Tables S1-3). Like the dry skull method, other muscles show
201 qualitatively variable error in the AA analysis across the three morphotypes; the anterior deep
202 masseter PCSA is underestimated in the rat but overestimated in the squirrel and guinea pig. The
203 infraorbital and posterior zygomatico-mandibularis muscles also show qualitatively different error
204 across the studied taxa (Fig 1, Tables S1-3). Our relatively large errors in predicted PCSAs are
205 qualitatively consistent with single taxon assessments of AA methods in humans [31-32] and
206 macaques [33-34]. These studies recovered weak, and in some instances statistically insignificant,
207 correlations between jaw muscle PCSA and a range of linear and area osteological attachment
208 proxies and concluded that predictive relationships had considerable error margins [31-34].
209 However, these studies did not investigate the consequences of such error margins for functional
210 metrics like bite force or bone loading.

211

212 Our findings highlight that the size of a muscle accommodation within or attachment area on the

213 cranium is not necessarily a reliable guide to muscle PCSA, and that MAA-based approaches
214 cannot necessarily be relied upon to produce systematic quantitative or even qualitative error across
215 homologous muscles in different species (Fig 1). This is further reflected in the relatively low
216 frequency with which they correctly order the relative PCSAs of homologous muscles across the
217 rodent morphotypes (the AA approach 10 out of 25 times; the dry skull method 1 out of 6 times). This
218 level of relative accuracy given by the AA method lies towards the lower end of the range that
219 Broyde et al. [36] recovered in these same three rodent specimens using muscle volume sculpture
220 reconstruction. Using volume sculpture, one investigator recovered 29% accuracy in the relative
221 ordering of muscle PCSA in these rodents, while two other investigators independently yielded
222 63% and 75% accuracy [36].

223

224 Sensitivity or parameter-specific error tests are relatively commonplace in both MDA and FE
225 modelling studies [e.g. 38-39, 41-42, 49-58]. These studies provide a fundamental basis for
226 understand the absolute and relative impact of individual parameters on model predictions, thereby
227 indicating which anatomical and physiological input variables must be most appropriately defined
228 to ensure maximal model accuracy. Our anatomical reconstructions (Fig. 1) provide a new basis to
229 examine the sensitivity of bite force and bone loading predictions specifically associated with MAA
230 methods and macroevolutionary hypothesis testing (Fig 2-3). Our MAA-based MDA models
231 underestimated bite force in all three rodent morphotypes (Fig 2a-b), which is qualitatively similar
232 to the findings of previous evaluations of the dry skull method [1, 29-30], except Davis et al. [31]
233 who concluded that this approach accurately estimated bite forces in bats despite inaccurately
234 predicting muscle parameters. However, the magnitude of underestimation varied considerably
235 between rodent taxa (Fig 2a-b). The AA models incorrectly predicted a higher incisor bite force in
236 the guinea pig than the rat, while the dry skull method predicted the lowest bite force for the
237 squirrel instead of the highest (Fig 2a-b). These quantitative and qualitative errors warn against
238 simply applying uniform correction factors or elevated values for maximum isometric stress to

239 compensate for potential underestimation of bite force by MAA-based approaches [2-3, 6, 21].

240

241 Given mechanical efficiency is defined as the ratio between bite force and one of its major
242 determinants, summed muscle force, it might be expected that this parameter would show very
243 minor sensitivity to errors in PCSA (Fig 1). In some model iterations this does indeed appear to be
244 the case (Fig 2). However, larger errors in mechanical efficiency (>20%) are seen where relatively
245 large PCSA errors are focused in muscles with particularly small or large moments arms, such as
246 the AA iteration of the squirrel model (Fig 2, Tables S5-7). Furthermore, this means that absolute or
247 even relative error in mechanical efficiency is not predictable from error in PCSA or bite force
248 alone: the summed muscle force and bite force are lower in AA model of the guinea pig than the
249 extant model (Fig 2a-b) iteration, yet mechanical efficiency is recovered as slightly higher in the
250 AA iteration (Fig 2c-d). Mechanical efficiency is considered a crucial functional adaptation that
251 distinguishes sciuriform, hystricomorph and myomorph rodents: squirrels (sciuriform
252 morphotype) are considered more efficient at muscle-bite force transmission during incisor gnawing
253 than guinea pigs (hystricomorph morphotype), which matches the known diet of nuts and seeds that
254 squirrel gnaw, and of grasses that guinea pigs grind down with their molars [46] (Fig 2c). Rats
255 (myomorph morphotype) are considered high performance generalists due to their high mechanical
256 efficiency in both incisor and molar biting [46] (Fig 2c). Because mechanical efficiency is similarly
257 underestimated in all taxa, the dry skull method recovers the adaptive pattern correctly, although the
258 distinction between squirrel and the rat is somewhat exaggerated relative to the extant model
259 iteration (Fig 2c). However, the AA method fails to recover this fundamental macroevolutionary
260 signal: the squirrel is recovered with the lowest efficiency in incisor biting (Fig 2c) and thus would
261 be incorrectly interpreted as lacking the aforementioned adaptation for incisor gnawing of hard food
262 types [46]. This might subsequently result in erroneous interpretations of the selective pressures
263 driving the radiation of rodent macroevolutionary morphotypes. The majority of volume sculpture
264 models of Broyde et al. [36] perform qualitatively and quantitatively better than MAA methods in

265 mechanical efficiency (Fig 2c-d). However, the potential for some erroneous interpretation of
266 inefficient incisor biting in the squirrel is also evident in the volume sculpture models of
267 investigator 3 (VS – 3a-c; Fig 2c).

268

269 To our knowledge, this study is the first to directly assess the accuracy with which MAA-based
270 approaches produce quantitative and qualitative patterns of bone stress in FE models across a
271 macroevolutionary radiation (Fig 3). Our results demonstrate that even the most basic or gross
272 pattern of stress distribution typically observed in mammalian skulls (higher stress in the central
273 skull regions in the zygomatic arch due to the attachment of large muscles to this relatively slender
274 rod-like process) may not be recovered by FE models loaded with MAA-based muscle forces (Fig
275 3a, c-d). While gross qualitative changes in stress along skull length are captured reasonably well in
276 the rat and guinea pig models, relative patterns are more poorly captured in the squirrel models
277 where stress remains much more uniform (Fig 3). MAA-based models also fail to recover major
278 qualitative differences between the morphotypes. For example, these models predict that the rat
279 experiences the lowest stresses (instead of the highest) of the three species and fail to recover stress
280 differences in zygomatic arch and posterior portion of the skull of models loaded with measured
281 muscle data presented by Broyde et al. [36,48] and Cox et al. [46-47]. Recovery of highest stresses
282 in the rat and lowest stresses in the guinea pig when models are loaded with measured muscle data
283 are consistent with osteological and muscular differences between the myomorph and
284 hystricomorph conditions. Rats (myomorph) have a large muscle mass to skull volume ratio,
285 particularly in the zygomatic arch, orbital wall and temporal regions where the relatively large
286 temporalis muscle of the rat generates higher stresses than are seen in the squirrel and guinea pig
287 skulls [36,46-47] (Fig 3d). In contrast, guinea pigs (hystricomorph) have relatively low overall
288 muscle mass for their skull size, but also possess a more robust morphology of the zygomatic arch
289 leading to lower stresses [36,46-47] (Fig 3d). The failure to capture these qualitative adaptive
290 differences, and indeed the relatively poor performance of the MAA-based models overall, is a

291 stark contrast to the accuracy of the volume sculpture model iterations presented by Broyde et al.
292 [36,48], where the majority of models produced qualitatively accurate stress predictions and some
293 iterations yielded extremely accurate quantitative predictions (Fig 3c, Fig S8). Indeed, even the
294 worst qualitatively performing volume sculpture model out-performs the MAA-based models
295 presented here (Fig 3c, Fig S8).

296

297 Herein we have evaluated the quantitative and qualitative accuracy of MAA approaches relative to
298 other biomechanical models (Figs 2-3) in which nearly all muscle parameters were measured
299 directly from the cadaveric specimens being modelled [43, 46-47]. Given the relatively simple
300 anatomical and functional activity under study (static maximal biting) it is likely that our 'extant
301 model' iterations represent good approximations of reality and suitable benchmarks against which
302 to measure the performance of MAA-based approaches in the context of macroevolutionary
303 research. However, use of a model (even one predominantly composed of species-specific input
304 data) as a benchmark for other models would clearly be less appropriate in other circumstances.
305 These might include, for example, more morphologically and functional complex situations (e.g.
306 predictive whole-body simulations of locomotion with multiple bodies, linked by joints with higher
307 degrees of freedom, controlled by large numbers of uni- and bi-articular muscles and interaction of
308 several contact bodies with an environment). However, given our focus on static maximal incisor
309 biting and the level of specimen-specific input data in our extant model iterations, we feel it is
310 extremely unlikely that our quantitative and qualitative conclusions about the accuracy of MAA
311 approaches would be altered by comparison to experimental data.

312

313 The extent to which the magnitudes of quantitative and qualitative error recovered here (Figs 1-3)
314 limit their predictive capability of MAA approaches is likely to vary according to the taxa and
315 hypotheses under study. However, these results strongly suggest that MAA-based approaches are

316 unlikely to accurately reproduce macroevolutionary changes in muscle proportions or
317 biomechanical performance with high fidelity. Perhaps with the exception of mechanical efficiency
318 (Fig 2c-d), quantitative errors are consistently high and qualitative error is commonplace, resulting
319 in the loss of anatomically and functionally defining features within individual species and
320 erroneous conclusions about relative adaptations across rodent macroevolutionary morphotypes. It
321 is currently rare for analyses of anatomical and functional evolution using MAA methods to
322 formally acknowledge error in their hypothesis testing. Our results provide clear evidence of the
323 need for this to become standard practice in order to objectively test or demonstrate the predictive
324 capability of MAA-based estimates in the context of the functional and macroevolutionary
325 hypotheses they have been constructed to test. In palaeontological studies, high levels of
326 quantitative error may always persist due to need to reconstructively estimate most, if not all, force-
327 generating muscle properties. However, error testing on extant taxa and the application of the
328 resulting error margins to predictions of extinct taxa provides at least indirect evaluation of the
329 predictive capabilities of models and their ability to provide meaningful tests of functional
330 hypotheses [36, 41-42,48-50]. Such studies also help to identify which parameters currently limit
331 the predictive capabilities of models, and thus where future research investment in generating new
332 methods and data might be best focused. The magnitudes of quantitative error and frequency of
333 qualitative or relative error across models seen here (Figs 1-3) suggests that current MAA methods
334 do not represent a legitimate means to achieve the 3Rs in biomechanical studies of extant taxa.
335 While a universal benchmark for model accuracy does not exist, it could be argued that near
336 unanimous success in predicting relative or qualitative anatomical and functional differences
337 between species or morphotypes represents a minimum threshold for a modelling method to serve
338 as a valid alternative to direct experimentation on animals. If such were achieved, modelling
339 approach could be used instead of experimentation to test certain hypotheses about relative
340 differences between species and qualitative cause-effect relationships in their functional anatomy.
341 Unfortunately, our results suggest that MAA methods may, at present, fall short of that benchmark.

342

343 It seems clear that the failing of current MAA-based approaches comes from the assumption of a
344 one-to-one relationship between attachment area and PCSA in each muscle, which is clearly not the
345 case (Fig 1). An alternative, and perhaps predictively superior approach, would be to examine the
346 scaling relationship between MAA and gross properties (volume, PCSA) within homologous
347 muscles across a large number of species. Similar approaches are widely used for estimating body
348 mass based on various skeletal proportions [e.g. 59-60] and have the advantage of delivering
349 statistically-based estimates with confidence intervals that permit objective and systematic error
350 testing in subsequent biomechanical models [36, 41-42,48-50,58]. We therefore suggest that future
351 work should go back to the bones to test if large data sets can yield strong predictive relationships
352 between MAAs and muscle properties (volume, PCSA) for use in macroevolutionary and functional
353 studies.

354

355 **Author Contributions**

356 K.T.B. conceived the study. S.B., K.T.B., and P.G.C. designed the study. S.B., K.T.B., M.D., L.W.,
357 M.F., and P.G.C. collected the data and carried out the analyses. All authors contributed to the
358 manuscript.

359

360 **Acknowledgements**

361 Roger Kissane is thanked for assistance with Figure 1a.

362

363 **Data Accessibility**

364 All models are available from the Dryad Digital Repository:
365 <https://doi.org/10.5061/dryad.kd51c5b4c> and the University of Liverpool's DataCat
366 facility: <https://doi.org/10.17638/datacat.liverpool.ac.uk/1184>.

367

368

369 **Funding Statement**

370 This work was funded by a NERC standard grant (NE/ G001952/1) to P.G.C. and M.J.F., a BBSRC
371 responsive mode grant to M.F. and K.T.B. (nos. BB/R016380/1; BB/R016917/1; BB/ R017190/1)
372 and a NERC doctoral dissertation grant (nos. NE/ S00713X/1) to M.D.

373

374 **References**

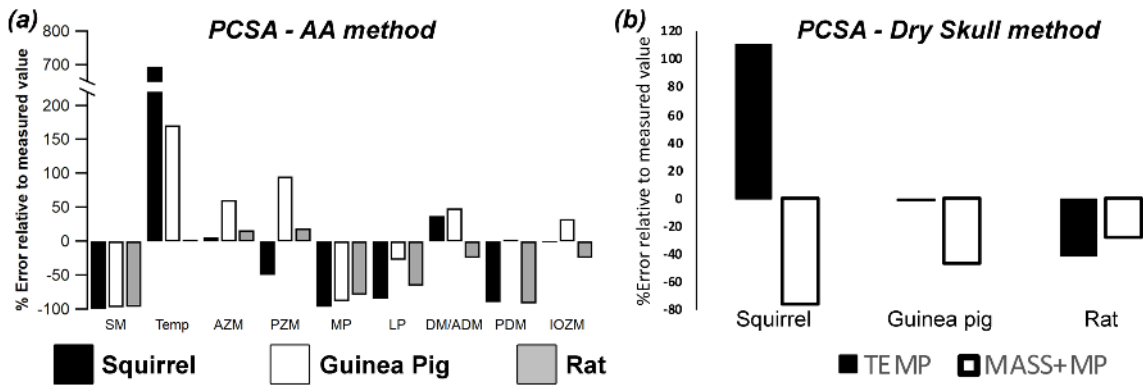
- 375 [1] Thomason JJ. 1991 Cranial strength in relation to estimated biting forces in some mammals.
376 *Canadian Journal of Zoology* **69**, 2326–2333.
377
- 378 [2] Christiansen P, Adolfssen JS. 1999 Bite forces, canine strength and skull allometry in carnivores
379 (Mammalia, Carnivora). *Journal of Zoology* **266**, 133–151.
380
- 381 [3] Christiansen P, Wroe S. 2007 Bite forces and evolutionary adaptations to feeding ecology in
382 carnivores. *Ecology* **88**, 347–358.
383
- 384 [4] Sakamoto M, Lloyd GT, Benton MJ. 2010 Phylogenetically structured variance in felid bite
385 force: The role of phylogeny in the evolution of biting performance. *Journal of Evolutionary*
386 *Biology* **23**, 463–478.
387
- 388 [5] Law CJ, Duran E, Hung N, Richards E, Santillan I, Mehta RS. 2018 Effects of diet on cranial
389 morphology and biting ability in musteloid mammals. *Journal of Evolutionary Biology* **31**, 1918–
390 1931.
391
- 392 [6] Wroe S, McHenry C, Thomason J. 2005 Bite club: Comparative bite force in big biting
393 mammals and the prediction of predatory behaviour in fossil taxa. *Proceedings of the Royal Society*
394 *B* **272**, 619–625.
395
- 396 [7] Jasinowski SC, Rayfield EJ, Chinsamy A. 2010 Functional implications of dicynodont cranial
397 suture morphology. *Journal of Morphology* **271**, 705–728.
398
- 399 [8] Jasinowski SC, Rayfield EJ, Chinsamy A. 2010 Mechanics of the scarf premaxilla-nasal suture in
400 the snout of *Lystrosaurus*. *Journal of Vertebrate Paleontology* **30**, 1283–1288.
401

- 402 [9] Jasinowski SC, Rayfield EJ, Chinsamy A. 2009 Comparative feeding biomechanics of
403 Lystrosaurus and the generalized dicynodont *Oudenodon*. *Anatomical Record: Advances in*
404 *Integrative Anatomy and Evolutionary Biology* **292**, 862-874.
- 405
- 406 [10] Lautenschlager S, Figueirido B, Cashmore D, Bendel EM, Stubbs T. 2020 Morphological
407 convergence obscures functional diversity in sabre-toothed carnivores. *Proceedings of the Royal*
408 *Society B* **287**, 20201818.
- 409
- 410 [11] Montefeiro F, Lautenschlager S, Godoy P, Ferreira G, Butler R. 2020 A unique predator in a
411 unique ecosystem: modelling the apex predator within a Late Cretaceous crocodyliform-dominated
412 fauna from Brazil. *Journal of Anatomy* **237**, 323-333.
- 413
- 414 [12] Ferreira G, Lautenschlager S, Evers S, Pfaff C, Kriwet J, Raselli I, Werneburg I. 2020 Feeding
415 biomechanics suggests progressive correlation of skull architecture and neck evolution in
416 turtles. *Scientific Reports* **10**, 5505.
- 417
- 418 [13] Figueirido B, Lautenschlager S, Pérez-Ramos A, Van Valkenburgh B. 2018 Distinct predatory
419 behaviors in scimitar- and dirk-toothed sabertooth cats. *Current Biology* **28**, 3260–3266.e3.
- 420
- 421 [14] Lautenschlager S, Witzmann F, Werneburg I. 2016 Palate anatomy and morphofunctional
422 aspects of interpterygoid vacuities in temnospondyl cranial evolution. *Naturwissenschaften* **103**, 79.
- 423
- 424 [15] Oldfield CC, McHenry CR, Clausen PD, Chamoli U, Parr WCH, Stynder DD, Wroe S. 2012.
425 Finite Element Analysis of ursid cranial mechanics and the prediction of feeding behaviour in the
426 extinct giant *Agriotherium africanum*. *Journal of Zoology* **286**, 163-170.
- 427
- 428 [16] Wroe S, Ferrara T, McHenry C, Curnoe D, Chamoli U. 2010 The craniomandibular mechanics
429 of being human. *Proceedings of the Royal Society B* **277**, 3579-3586.
- 430
- 431 [17] Wroe S, Milne N. 2007 Convergence and remarkably consistent constraint in the evolution of
432 carnivore skull shape. *Evolution* **61**, 1251-1260.
- 433
- 434 [18] Snively E, Fahlke JM, Welsh RC. 2015 Bone-breaking bite force of *basilosaurus isis*
435 (mammalia, cetacea) from the late eocene of Egypt estimated by finite element analysis
436 e0118380. *PLoS ONE* **10**(2), <https://doi.org/10.1371/journal.pone.0118380>.
- 437
- 438 [19] Bell PR, Snively E, Shychoski L. 2009 A comparison of the jaw mechanics in hadrosaurid and
439 ceratopsid dinosaurs using finite element analysis. *Anatomical Record* **292**, 1338-1351.
- 440
- 441 [20] Serrano-Fochs S, De Esteban-Trivigno S, Marcé-Nogué J, Fortuny J, Fariña RA. 2015 Finite
442 element analysis of the Cingulata jaw: an ecomorphological approach to armadillo's diets. *PLoS*
443 *ONE*, <https://doi.org/10.1371/journal.pone.0120653>
- 444
- 445 [21] Sakamoto M, Ruta M, Venditti C. 2019 Extreme and rapid bursts of functional adaptations
446 shape bite force in amniotes. *Proceedings of the Royal Society B* **286**, 20181932.
- 447
- 448 [22] Snively E, O'Brien H, Henderson DM, Mallison H, Surring LA, Burns ME, Holtz TR, Russell
449 AP, Witmer LM, Currie PJ, Hartman SA, Cotton JR. 2019 Lower rotational inertia and larger leg
450 muscles indicate more rapid turns in tyrannosaurids than in other large theropods. *PeerJ*, 2019(2),
451 [e6432] <https://doi.org/10.7717/peerj.6432>
- 452

- 453 [23] Fahn-Lai P, Biewener AA, Pierce SE. 2020 Broad similarities in shoulder muscle architecture
454 and organization across two amniotes: implications for reconstructing non-mammalian
455 synapsids. *PeerJ* **8**, e8556.
456
- 457 [24] Rhodes MM, Henderson DM, Currie PJ. 2021. Maniraptoran pelvic musculature highlights
458 evolutionary patterns in theropod locomotion on the line to birds. *PeerJ* **9**, e10855.
459
- 460 [25] Snively E, Cotton JR, Ridgely R, Witmer LM. 2013 Multibody dynamics model of head and
461 neck function in *Allosaurus* (Dinosauria, Theropoda). *Palaeontologia*
462 *Electronica*, **16**(2). <https://doi.org/10.26879/338>
463
- 464 [26] Snively E, Russell AP. 2007 Craniocervical feeding dynamics of *Tyrannosaurus*
465 *rex*. *Paleobiology* **33**, 610-638.
466
- 467 [27] McHenry C, Wroe S, Clausen P, Moreno K, Cunningham E. 2007 Super-modeled sabercat,
468 predatory behaviour in *Smilodon fatalis* revealed by high-resolution 3-D computer simulation.
469 *Proceedings of the National Academy of Sciences USA*, **104**, 16010-16015.
470
- 471 [28] Russell WMS, Burch RL. 1959. The Principles of Humane Experimental Technique. Methuen,
472 London (UK).
473
- 474 [29] Law CJ, Mehta RS. 2019 Dry versus wet and gross: Comparisons between the dry skull
475 method and gross dissection in estimations of jaw muscle cross-sectional area and bite forces in sea
476 otters. *Journal of Morphology* **280**, 1706–1713.
477
- 478 [30] Ellis JL, Thomason JJ, Kebreab E, France J. 2008 Calibration of estimated biting forces in
479 domestic canids: Comparison of post-mortem and in vivo measurements. *Journal of Anatomy* **212**,
480 769–780.
481
- 482 [31] Toro-Ibacache V, Zapata Muñoz V, O'Higgins P. 2015 The predictability from skull
483 morphology of temporalis and masseter muscle cross-sectional areas in humans. *The Anatomical*
484 *Record* **298**, 1261-1270.
485
- 486 [32] Antón SC. 1994 Masticatory muscle architecture and bone morphology in primates. Berkeley,
487 CA: University of California.
488
- 489 [33] Antón SC. 1999 Macaque masseter muscle: internal architecture, fiber length and cross-
490 sectional area. *International Journal of Primatology* **20**, 441-462.
491
- 492 [34] Antón SC. 2000 Macaque pterygoid muscles: internal architecture, fiber length, and cross-
493 sectional area. *International Journal of Primatology* **21**, 131-156.
494
- 495 [35] Davis JL, Santana SE, Dumont ER, Grosse IR. 2010 Predicting bite force in mammals: Two-
496 dimensional versus three-dimensional lever models. *The Journal of Experimental Biology* **213**,
497 1844–1851.
498
- 499 [36] Broyde S, Dempsey M, Wang L, Cox PG, Fagan M, Bates KT. 2021 Evolutionary
500 biomechanics: hard tissues and soft evidence? *Proceedings of the Royal Society B* **288**, 20202809.
501
- 502 [37] Persons WS, Currie PJ. 2011 The tail of *Tyrannosaurus*: reassessing the size and locomotive
503 importance of the M. caudofemoralis in non-avian theropods. *The Anat. Rec.* **294**, 119–131.
504

- 505 [38] Bates KT, Benson, RBJ, Falkingham PL. 2012 The evolution of body size, stance and gait in
506 Allosauroidea (Dinosauria: Theropoda). *Paleobiology* **38**, 486-507.
507
- 508 [39] Allen V, Bates, KT, Zhiheng L, Hutchinson JR. 2013 Linking the evolution of body shape and
509 locomotor biomechanics in bird-line archosaurs. *Nature* **497**, 104-107.
510
- 511 [40] Gignac PM, Erickson GM. 2017 The biomechanics behind extreme osteophagy in
512 *Tyrannosaurus rex*. *Scientific Reports* DOI: 10.1038/s41598-017-02161-w.
513
- 514 [41] Bates KT, Falkingham PL. 2012 Estimating maximum bite performance in *Tyrannosaurus rex*
515 using multi-body dynamics. *Biology Letters* **8**, 660-664.
516
- 517 [42] Bates KT, Falkingham PL. 2018 The importance of muscle architecture in biomechanical
518 reconstructions of extinct animals: a case study using *Tyrannosaurus rex*. *Journal of Anatomy*. **233**,
519 625-635.
520
- 521 [43] Cox PG, Jeffery N, 2015 The muscles of mastication in rodents and the function of the medial
522 pterygoid. In: *Evolution of the Rodents: Advances in Phylogeny, Functional Morphology and*
523 *Development* (eds PG Cox, L Hautier). Cambridge: Cambridge University Press, pp 350-372.
524
- 525 [44] Hautier L, Cox PG, Lebrun R. 2015 Grades and clades among rodents: the promise of
526 geometric morphometrics. In: *Evolution of the Rodents: Advances in Phylogeny, Functional*
527 *Morphology and Development* (eds PG Cox, L Hautier). Cambridge: Cambridge University Press,
528 pp 277-299.
529
- 530 [45] Wood AE. 1965 Grades and clade among rodents. *Evolution* **19**,115-130.
531
- 532 [46] Cox PG, Rayfield EJ, Fagan MJ, Herrel A, Pataky TC, Jeffery N. 2012 Functional evolution of
533 the feeding system in rodents. *PLoS ONE* **7**(4), e36299.
534
- 535 [47] Cox PG, Fagan MJ, Rayfield EJ, Jeffery N. 2011 Biomechanical performance of squirrel,
536 guinea pig and rat skulls: sensitivity analyses of finite element models. *Journal of Anatomy* **219**:
537 696-709.
538
- 539 [48] Broyde, S., Dempsey, M., Wang, L., Cox, P.G., Fagan, M. & Bates, K.T. 2021. Correction to
540 ‘Evolutionary biomechanics: hard tissues and soft evidence?’ *Proceedings of the Royal Society B*.
541 <https://doi.org/10.1098/rspb.2021.0831>.
542
- 543 [49] Bates KT, Manning PL, Margetts L, Sellers WI. 2010 Sensitivity analysis in evolutionary
544 robotic simulations of bipedal dinosaur running. *Journal of Vertebrate Paleontology* **30**, 458-466.
545
- 546 [50] Hutchinson, J.R. 2012. On the inference of function from structure using biomechanical
547 modelling and simulation of extinct organisms. *Biology Letters* **8**, 115–118.
548
- 549 [51] Ross CF, Patel BA, Slice DE, Strait DS, Dechow PC, Richmond BG, et al. 2005 Modeling
550 masticatory muscle force in finite element analysis: sensitivity analysis using principal coordinates
551 analysis. *The Anatomical Record* **283**, 288-99.
552
- 553 [52] Kupczik K, Dobson CA, Fagan MJ, Crompton RH, Oxnard CE, O’Higgins P. 2007 Assessing
554 mechanical function of the zygomatic region in macaques: validation and sensitivity testing of finite
555 element models. *Journal of Anatomy* **210**, 41-53.
556

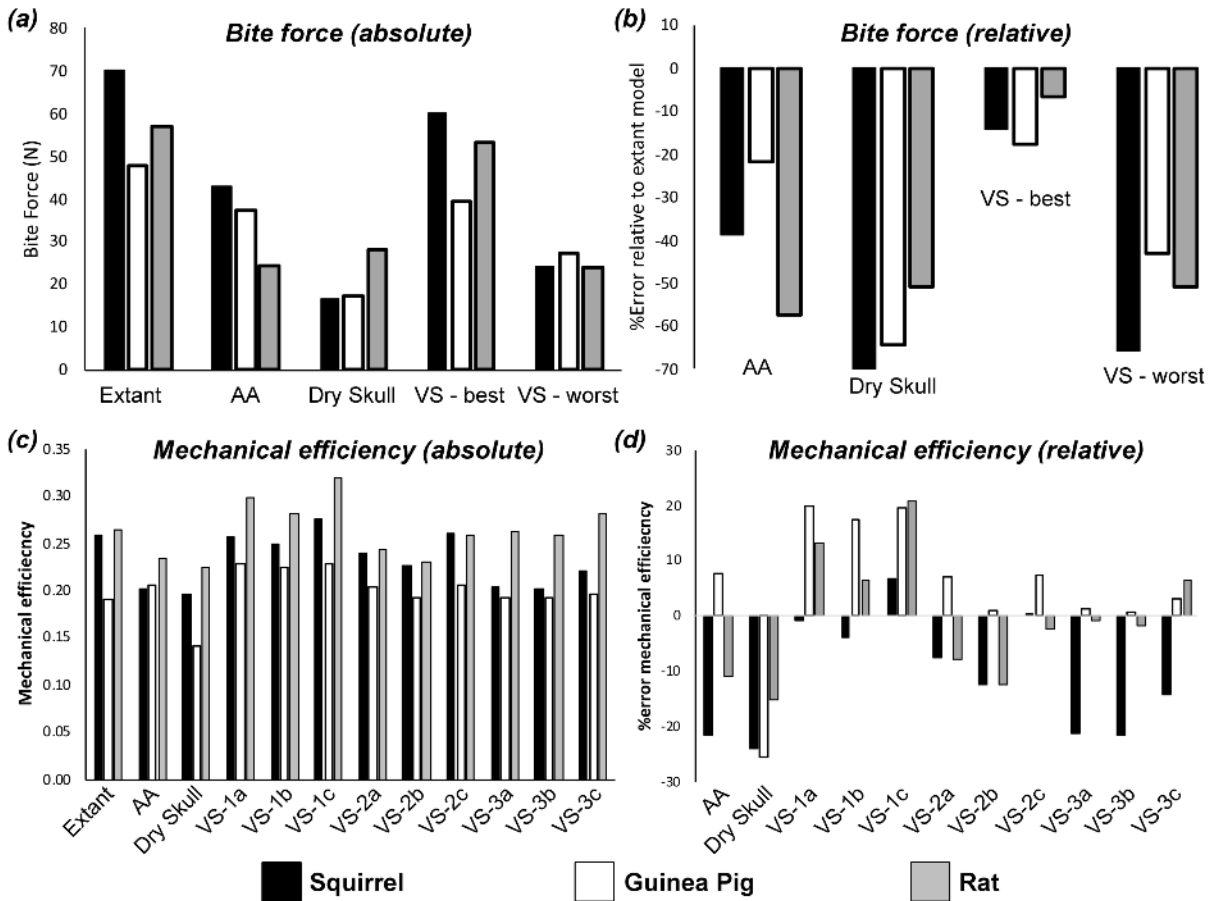
- 557 [53] Tseng ZJ, McNitt-Gray JL, Flashner H, Wang X, Enciso R. 2011 Model Sensitivity and Use of
558 the Comparative Finite Element Method in Mammalian Jaw Mechanics: Mandible Performance in
559 the Gray Wolf. *PLoS ONE* **6**:e19171.
560
- 561 [54] Fitton LC, Shi JF, Fagan MJ, O'Higgins P. 2012 Masticatory loadings and cranial deformation
562 in *Macaca fascicularis*: a finite element analysis sensitivity study. *Journal of Anatomy* **221**, 55-68.
563 [55] Gröning F, Fagan MJ, O'Higgins P. 2012. Modeling the human mandible under masticatory
564 loads: which input variables are important? *The Anatomical Record* **295**, 853-63.
565
- 566 [56] Toro-Ibacache V, O'Higgins P. 2016 The Effect of Varying Jaw-elevator Muscle Forces on a
567 Finite Element Model of a Human Cranium. *The Anatomical Record* **299**, 828-39.
568
- 569 [57] Stansfield E, Parker J, O'Higgins P. 2018 A sensitivity study of human mandibular biting
570 simulations using finite element analysis. *Journal of Archaeological Science: Reports* **22**, 420-432.
571
- 572 [58] Cox PG, Rinderknecht A, Blanco RE. 2015 Predicting bite force and cranial biomechanics in
573 the largest fossil rodent using finite element analysis. *Journal of Anatomy* **226**, 215-223.
574
- 575 [59] Sellers WI, Hepworth-Bell J, Falkingham PL, Bates KT, Brassey C, Egerton V, Manning PL.
576 2012 Minimum convex hull mass estimations of complete mounted skeletons. *Biology Letters* **8**:
577 842-845.
578
- 579 [60] Campione NE, Evans DC. 2012 A universal scaling relationship between body mass and
580 proximal limb bone dimensions in quadrupedal terrestrial tetrapods. *BMC Biology* **10**, 60.
581
582
583



584
585
586
587
588
589

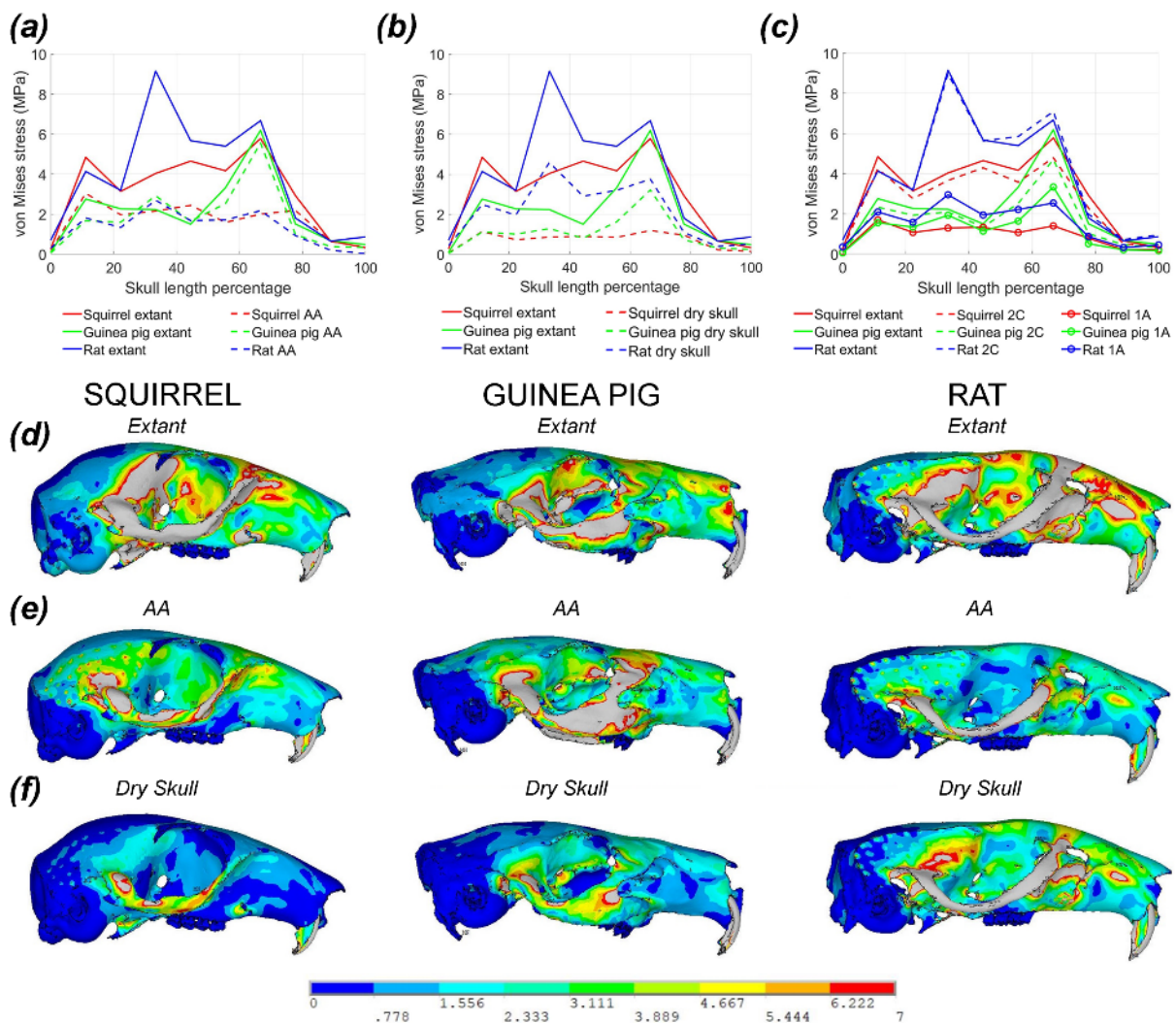
Figure 1. Relative error in PCSA given by *(a)* the attachment area (AA) and *(b)* the dry skull method. Error magnitudes represent the percentage error in the AA and dry skull values relative to the measured PCSA values in the rodent specimens being modelled [43,46-47].

590



591
 592
 593
 594
 595
 596
 597
 598
 599
 600

Figure 2. Absolute values and relative error in maximal incisor (*a-b*) bite force and (*c-d*) mechanical efficiency in MDA models built using PCSAs from the AA and dry skull method compared to extant MDA model iterations, and those generated previously using the volumetric sculpture (VS) approach [36]. Error magnitudes in (*b*) and (*d*) represent the percentage error in the AA, dry skull and/or volumetric sculpture values relative to the to the extant MDA model bite force and mechanical efficiency values for each taxon [36, 46-47].



601
 602 **Figure 3.** Comparison of stress magnitudes and distributions (represented by von Mises stress)
 603 along the length of the skull in the FE model iterations loaded using muscle properties measured in
 604 the rodent specimens being modelled (the extant model iterations) to model iterations where muscle
 605 properties were derived from (a) the AA method, (b) dry skull method, and (c) muscle volume
 606 sculpture. In (c) only the most (2C) and least (1A) accurate iterations of the volume sculpture
 607 models from [36,48] are shown for comparative purposes. (d-f) Visualisation of von Mises stress
 608 contour plots on the skulls themselves highlights the error in relative and absolute stress predicted
 609 in the (e) AA and (f) dry skull models versus to the (d) extant model iterations, particularly along
 610 the zygomatic arch.

611
 612